

# A Density Matrix Algorithm for 3D Classical Models

Tomotoshi NISHINO\* and Kouichi OKUNISHI<sup>1,\*\*</sup>

*Department of Physics, Faculty of Science, Kobe University, Rokkodai 657-8501*

<sup>1</sup>*Department of Physics, Graduate School of Science, Osaka University, Toyonaka 560-0043*

(Received )

We generalize the corner transfer matrix renormalization group, which consists of White's density matrix algorithm and Baxter's method of the corner transfer matrix, to three dimensional (3D) classical models. The renormalization group transformation is obtained through the diagonalization of density matrices for a cubic cluster. A trial application for 3D Ising model with  $m = 2$  is shown as the simplest case.

KEYWORDS: Density Matrix, Renormalization Group, Corner Tensor.

## §1. Introduction

Variational estimation of the partition function has been one of the standard technic in statistical mechanics. For a two-dimensional (2D) classical lattice model defined by a transfer matrix  $T$ , the variational partition function per row is written as

$$\lambda = \frac{\langle V | T | V \rangle}{\langle V | V \rangle}, \quad (1.1)$$

where  $|V\rangle$  represents the trial state and  $\langle V|$  is its conjugate;  $\lambda$  is maximized when  $\langle V|$  and  $|V\rangle$  coincide with the left and the right eigenvectors of  $T$ , respectively. In 1941 Klamers and Wannier<sup>1,2)</sup> investigated the Ising model, assuming that  $|V\rangle$  is well approximated by a product of matrices

$$V(\dots, i, j, k, l, \dots) = \dots F^{ij} F^{jk} F^{kl} \dots, \quad (1.2)$$

where  $i, j, k, l$ , etc., are the Ising variables, and  $F^{ij}$  is a symmetric 2 by 2 matrix. The approximation is more accurate than both the mean-field and the Bethe approximations.<sup>3)</sup> Baxter improved the trial state by introducing additional degrees of freedom.<sup>4,5,6)</sup> His variational state is defined as

$$V(\dots, i, j, k, l, \dots) = \sum_{\dots, a, b, c, d, \dots} \dots F_{ab}^{ij} F_{bc}^{jk} F_{cd}^{kl} \dots, \quad (1.3)$$

---

\* e-mail: nishino@phys560.phys.kobe-u.ac.jp

\*\* e-mail: okunishi@godzilla.phys.sci.osaka-u.ac.jp

where  $a, b, c, d$ , etc., are  $2^n$ -state group spin variables. The tensor  $F_{ab}^{ij}$  contains  $4 \cdot 2^{2n}$  elements, and therefore it is not easy to optimize  $F_{ab}^{ij}$  — adjust the elements — so that  $\lambda$  is maximized. He solved the optimization problem by introducing the corner transfer matrix (CTM), and by solving self-consistent equations for the tensors.<sup>6)</sup> In 1985 Nightingale and Blöte used Baxter's tensor product as a initial state in the projector Monte Carlo simulation for the Haldane system.<sup>7)</sup> Baxter suggested an outline of generalizing his CTM method to 3D systems,<sup>6)</sup> however, the project has not been completed.

Similar variational formulations have been applied to one-dimensional (1D) quantum systems, especially for  $S = 1$  spin chains. The variational ground state  $|\Psi\rangle$  is given by a modified tensor product

$$\Psi(\dots, i, j, k, l, \dots) = \sum_{\dots, a, b, c, d, e, \dots} \dots A_{ab}^i A_{bc}^j A_{cd}^k A_{de}^l \dots, \quad (1.4)$$

where the subscripts  $a, b, c, d, e$ , etc., are  $m$ -state group spin variables. Affleck, Lieb, Kennedy, and Tasaki (AKLT) showed that the ground-state of a bilinear-biquadratic  $S = 1$  spin chain is exactly expressed by the tensor product with  $m = 2$ .<sup>8)</sup> The variational formulation has been generalized by Fannes et. al. for the arbitrary large  $m$ .<sup>9,10,11)</sup> Now such ground state is called ‘finitely correlated state’<sup>10)</sup> or ‘matrix product state’.<sup>12)</sup> Quite recently Niggemann et. al.<sup>13)</sup> showed that the ground state of a 2D quantum systems can be exactly written in terms of a two-dimensional tensor product. Although  $|\Psi\rangle$  in Eq.(1.3) does not look like  $|V\rangle$  in Eq.(1.4), they are essentially the same. We can transform  $|V\rangle$  into  $|\Psi\rangle$  by obtaining  $A_{ab}^i$  from  $F_{ab}^{ij}$  through a kind of duality transformation,<sup>14)</sup> the opposite is also possible.

The application of both  $|V\rangle$  in Eq.(1.3) and  $|\Psi\rangle$  in Eq.(1.4) are limited to translationally invariant (or homogeneous) systems. In 1992 White established a more flexible numerical variational method from the view point of the real-space renormalization group (RG).<sup>15,16)</sup> Since his numerical algorithm is written in terms of the density matrix, the algorithm is called ‘density matrix renormalization group’ (DMRG). White's variational state is written in a position dependent tensor product<sup>17,18)</sup>

$$\Phi(\dots, i, j, k, l, \dots) = \sum_{\dots, a, b, c, d, e, \dots} \dots A_{ab}^i B_{bc}^j C_{cd}^k D_{de}^l \dots, \quad (1.5)$$

where  $A_{ab}^i$  is not always equal to  $B_{ab}^i$ , etc. This inhomogeneous property in  $|\Phi\rangle$  makes DMRG possible to treat open boundary systems<sup>19)</sup> and random systems.<sup>20)</sup> Now the DMRG is widely used for both quantum<sup>21)</sup> and classical<sup>22,23,24)</sup> problems. Quite recently Dukelsky et. al. analyzed the correspondence (and a small discrepancy) between DMRG and the variational formula in Eq.(1.4).<sup>25,26,27)</sup>

The decomposition of the trial state into the tensor product tells us how to treat lattice models when we try to obtain the partition function. The essential point is to break-up the system into smaller pieces — like the local tensor  $F_{ab}^{ij}$  in Eq.(1.3) or  $A_{ab}^i$  in Eq.(1.4) — and reconstruct

the original system by multiplying them. According to this idea, the authors combine DMRG and Baxter's method of CTM, and proposed the corner transfer matrix renormalization group (CTMRG) method.<sup>28,29)</sup> It has been shown that CTMRG is efficient for determinations of critical indices<sup>29)</sup> or latent heats.<sup>30)</sup>

The purpose of this paper is to generalize the algorithm of CTMRG to three-dimensional (3D) classical systems. We focus on the RG algorithm rather than its practical use. In the next section, we briefly review the outline of CTMRG. The key point is that the RG transformation is obtained through the diagonalization of the density matrix. In §3 we define the density matrix for a 3D vertex model, and in §4 we explain the way to obtain the RG transformation. The numerical algorithm is shown in §5. A trial application with  $m = 2$  is shown for the 3D Ising Model. Conclusions are summarized in §6.

## §2. Formulation in Two Dimension

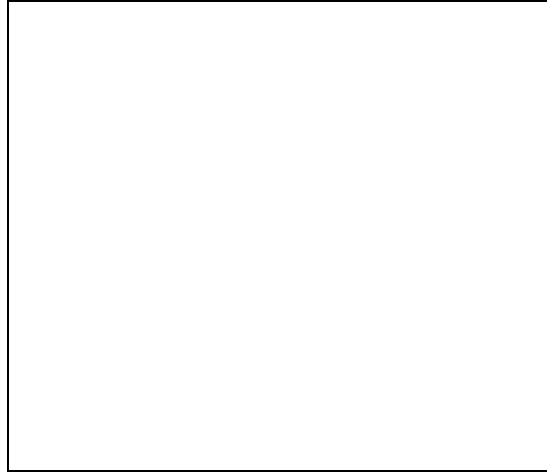


Fig. 1. Square cluster of a symmetric vertex model; the shown system is the example with linear dimension  $2N = 6$ . The cross marks  $\times$  show the boundary spins.

The aim of CTMRG is to obtain variational partition functions of 2D classical models. Let us consider a square cluster of a 16-vertex model (Fig.1) as an example of 2D systems. We impose the fixed boundary condition, where the boundary spins shown by the cross marks point the same direction. In order to simplify the following discussion, we assign a symmetric Boltzmann weight  $W_{ijkl} = W_{jkli} = W_{ilkj}$  to each vertex,<sup>31)</sup> where  $i, j, k$  and  $l$  denote two-state spins (= Ising spins or

arrows) on the bonds. (Fig.2(a))



Fig. 2. Boltzmann weight and transfer matrices. The dots represent spin variables inside the square cluster shown in Fig.1, and the cross marks represent the boundary spins. (a) Vertex weight  $W_{ijkl}$ . (b) Half-row transfer matrix  $P_{ab}^i$ . (c) Corner transfer matrix  $C_{ab}$ .

We employ two kinds of transfer matrices in order to express the partition function  $Z_{2N}$  of the square cluster with linear dimension  $2N$ . One is the half-row transfer matrix (HRTM). Figure 2(b) shows the HRTM  $P_{ab}^i$  with length  $N = 3$ , where the subscripts  $a = (a_1, a_2, \dots, a_N)$  and  $b = (b_1, b_2, \dots, b_N)$ , respectively, represent row spins — in-line spins — on the left and the right sides of the HRTM. We think of  $P_{ab}^i$  as a matrix labeled by the superscript  $i$ . The other is the Baxter's corner transfer matrix (CTM),<sup>4,5,6)</sup> that represents Boltzmann weight of a quadrant of the square. Figure 2(c) shows the CTM  $C_{ab}$  with linear dimension  $N = 3$ . The partition function  $Z_{2N}$  is then expressed as

$$Z_{2N} = \text{Tr } \rho = \text{Tr } C^4, \quad (2.1)$$

where  $\rho_{ab} \equiv (C^4)_{ab}$  is the density matrix. From the symmetry of the vertex weight  $W_{ijkl}$ , the matrices  $P_{ab}^i$ ,  $C_{ab}$ , and  $\rho_{ab}$  are invariant under the permutation of subscripts.

There are recursive relations between  $W$ ,  $P$ , and  $C$ . We can increase the length of HRTM by joining a vertex

$$P_{\bar{a}\bar{b}}^i = \sum_k W_{ijkl} P_{ab}^k, \quad (2.2)$$

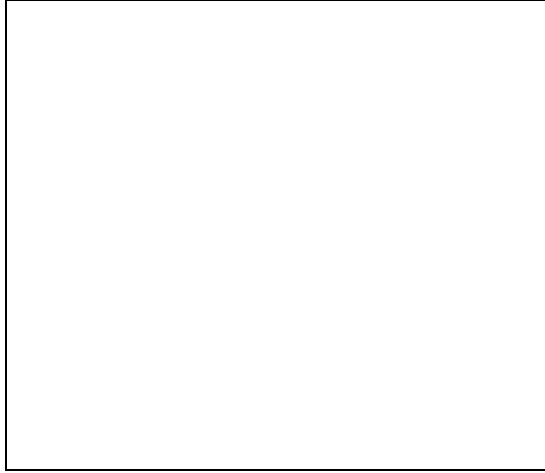


Fig. 3. Extensions of (a) the HRTM (Eq.(2.2)), and (b) the CTM. (Eq.(2.3))

where the extended row-spins are defined as  $\bar{a} = (a, l) = (a_1, a_2, \dots, a_N, l)$  and  $\bar{b} = (b, j) = (b_1, b_2, \dots, b_N, j)$ . (Fig.3(a)) In the same manner, the area of CTM can be extended by joining two HRTMs and a vertex to the CTM

$$C_{\bar{a}\bar{b}} = \sum_{cd\ kj} W_{ijkl} P_{db}^j P_{ac}^k C_{cd}, \quad (2.3)$$

where the extended row-spins  $\bar{a}$  and  $\bar{b}$  are defined as  $\bar{a} = (a, l) = (a_1, a_2, \dots, a_N, l)$  and  $\bar{b} = (b, i) = (b_1, b_2, \dots, b_N, i)$ . (Fig.3(b)) In this way, we can construct HRTM and CTM with arbitrary size  $N$  by repeating the extension Eqs.(2.2) and (2.3).

It should be noted that the matrix dimension of both  $C_{ab}$  and  $P_{ab}^i$  increases very rapidly with their linear size  $N$ . The fact prevents us to store the matrix elements of  $C_{ab}$  and  $P_{ab}^i$  when we numerically calculate the partition function  $Z_{2N}$ . This difficulty can be overcomed by compressing CTM and HRTM into smaller matrices via the density matrix algorithm,<sup>15,16)</sup> where the RG transformation is obtained through the diagonalization of the density matrix  $\rho_{ab} \equiv (C^4)_{ab}$ . Let us consider the eigenvalue equation for the density matrix

$$\sum_b \rho_{ab} A_b^\alpha = \lambda_\alpha A_a^\alpha, \quad (2.4)$$

where  $\lambda_\alpha$  is the eigenvalue in decreasing order  $\lambda_1 \geq \lambda_2 \geq \dots \geq 0$ , and  $\mathbf{A}^\alpha = (A_1^\alpha, A_2^\alpha, \dots)^T$  is the corresponding eigenvector that satisfies the orthogonal relation

$$(\mathbf{A}^\alpha, \mathbf{A}^\beta) = \sum_a A_a^\alpha A_a^\beta = \delta^{\alpha\beta}. \quad (2.5)$$

It has been known that  $\lambda_\alpha$  rapidly approaches to zero with respect to  $\alpha$ ,<sup>6,16)</sup> and that we can neglect tiny eigenvalues from the view point of numerical calculation. We consider only  $m$  numbers of dominant eigenvalues in the following; the greek indices run from 1 to  $m$ . The number  $m$  is determined so that  $\sum_{\alpha=1}^m \lambda_\alpha$  becomes a good lower bound for the partition function  $Z_{2N} = \text{Tr } \rho$ .

Equation (2.4) shows that for a sufficiently large  $m$  the density matrix  $\rho$  can be well approximated as

$$\rho_{ab} \sim \sum_{\alpha=1}^m A_a^\alpha A_b^\alpha \lambda_\alpha. \quad (2.6)$$

The above approximation shows that the  $m$ -dimensional diagonal matrix

$$\tilde{\rho}_{\alpha\beta} = \sum_{ab} A_a^\alpha A_b^\beta \rho_{ab} = \delta_{\alpha\beta} \lambda_\beta \quad (2.7)$$

contains the relevant information of  $\rho$ ; we can regard  $\tilde{\rho}$  as the renormalized density matrix. This is the heart of the density matrix algorithm: *the RG transformation is defined by the matrix  $A = (\mathbf{A}^1, \mathbf{A}^2, \dots, \mathbf{A}^m)$  which is obtained through the diagonalization of the density matrix.*

As we have applied the RG transformation to the density matrix  $\rho$ , we can renormalize the CTM by applying the matrix  $A$  as

$$\tilde{C}_{\alpha\beta} = \sum_{ab} A_a^\alpha A_b^\beta C_{ab}. \quad (2.8)$$

Since  $C_{ab}$  and  $\rho_{ab}$  have the common eigenvectors — remember that  $\rho = C^4$  — the renormalized CTM is an  $m$ -dimensional diagonal matrix

$$\tilde{C} = \text{diag}(\omega_1, \omega_2, \dots, \omega_m), \quad (2.9)$$

where  $\omega_\alpha$  is the eigenvalue of the CTM that satisfies  $\lambda_\alpha = \omega_\alpha^4$ . In the same manner, we obtain the renormalized HRTM

$$\tilde{P}_{\alpha\beta}^i = \sum_{ab} A_a^\alpha A_b^\beta P_{ab}^i. \quad (2.10)$$

In this case  $\tilde{P}_{\alpha\beta}^i$  is not diagonal with respect to  $\alpha$  and  $\beta$ ; *the RG transformation is not always diagonalization.*

We can extend the linear size of CTM and HRTM using Eqs.(2.2) and (2.3), and we can reduce their matrix dimension by the RG transformation in Eqs.(2.7) and (2.8). By repeating the extension and the renormalization, we can obtain the renormalized density matrix  $\tilde{\rho}$  and the approximate partition function  $\tilde{Z}_{2N} = \text{Tr } \tilde{\rho}$  for arbitrary system size  $N$ . This is the outline of the CTMRG.

### §3. Density matrix in Three Dimension

In order to generalize the density matrix algorithm to 3D systems, we first construct the density matrix in three dimension. As an example of 3D systems, we consider a 64-vertex model, that is defined by a Boltzmann weight  $W_{ijklmn}$ . (Fig.4(a)) In order to simplify the following discussion, we consider the case where  $W_{ijklmn}$  is invariant under the permutations of the two-state spins

$i, j, k, l, m$  and  $n$ .<sup>32)</sup> As we have considered a square cluster in two-dimension, (Fig.1) we consider a cube with linear dimension  $2N$ , where the boundary spins (on the surface of the cube) are fixed to the same direction. According to the variational formulation shown in §1, we first decompose the cube into several parts shown in Fig.4(b)-(d).

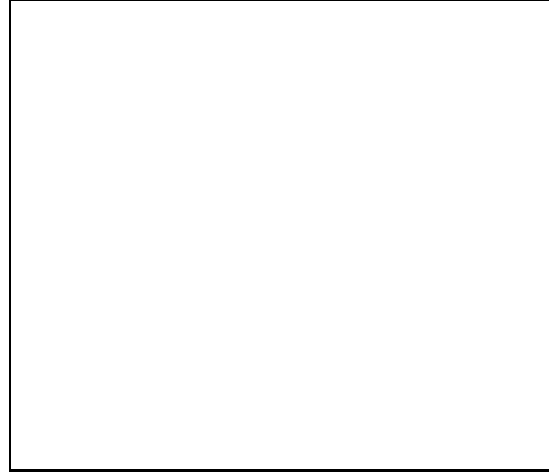


Fig. 4. Parts of the cubic cluster with linear dimension  $2N$ : (a) Vertex weight  $W_{ijklmn}$ . (b) The tensor  $P_{abcd}^i$ . (c) The tensor  $S_{ab}^{XY}$ . (d) Corner Tensor  $C^{XYZ}$ . The cross marks  $\times$  represent the boundary spins.

The tensor  $P_{abcd}^i$  shown in Fig.4(b) is a kind of three-dimensional HRTM. The superscript  $i$  represents the two-state spin at the top. The spin at the bottom is fixed, because it is at the boundary of the system. The subscript  $a$  represents the group of in-line spins  $a = (a_1, a_2, \dots, a_N)$ ;  $b$ ,  $c$ , and  $d$  are defined in the same way. From the symmetry of the vertex weight,  $P_{abcd}^i$  is invariant under the permutations of subscripts.

The tensor  $S_{ab}^{XY}$  shown in Fig.4(c) does not have its 2D analogue; it is an array of vertices. The subscripts  $a$  and  $b$  represent in-line spins; other two sides are the boundary of the cube. The superscript  $X$  represents an  $N$  by  $N$  array of spins on the square surface

$$X = \begin{pmatrix} x_{11} & x_{12} & \dots & x_{1N} \\ x_{21} & x_{22} & & \vdots \\ \vdots & & \ddots & \vdots \\ x_{N1} & \dots & \dots & x_{NN} \end{pmatrix}, \quad (3.1)$$

where  $x_{NN}$  is closest to the center of the cube, and  $Y$  is the spin array on the other surface;  $x_{ij}$

and  $y_{ij}$  are connected to the same vertex at the position  $\{ij\}$ . The tensor is invariant under the permutation of  $X$  and  $Y$  ( $S_{ab}^{XY} = S_{ab}^{YX}$ ), but is not invariant for  $a$  and  $b$  ( $S_{ab}^{XY} \neq S_{ba}^{XY}$ );  $S_{ab}^{XY}$  is equal to  $S_{ba}^{ZW}$  where  $Z = X^T$  and  $W = Y^T$ .

Figure 4(d) shows the corner tensor  $C^{XYZ}$ , which is a kind of three-dimensional CTM.<sup>6)</sup> The superscripts are defined in the same way as Eq.(3.1). (The boundary spins on the surfaces of the original cube are fixed.) It should be noted that  $C^{XYZ}$  is not equal to  $C^{WYZ}$  where  $W = X^T$ , because each surface has its own orientation.



Fig. 5. Extensions of (a)  $P$  in Eq.(3.2), (b)  $S$  in Eq.(3.3), and (c)  $C$  in Eq.(3.5).

Following the formulation in two-dimension, let us consider the size extension of  $P$ ,  $S$ , and  $C$ . The length of  $P$  can be increased by joining a vertex (Fig.5(a))

$$P_{\bar{a}\bar{b}\bar{c}\bar{d}}^{\bar{i}} = \sum_n W_{ijklmn} P_{abcd}^n, \quad (3.2)$$

where the extended in-line spins are defined as  $\bar{a} = (a, j) = (a_1, a_2, \dots, a_N, j)$ ,  $\bar{b} = (b, k) = (b_1, b_2, \dots, b_N, k)$ ,  $\bar{c} = (c, l) = (c_1, c_2, \dots, c_N, l)$ , and  $\bar{d} = (d, m) = (d_1, d_2, \dots, d_N, m)$ . The linear size of  $S$  can be increased by joining two  $P$  and a vertex (Fig.5(b))

$$S_{\bar{a}\bar{b}}^{\bar{X}\bar{Y}} = \sum_{ln} \sum_{ce} W_{ijklmn} P_{abcd}^n P_{efgh}^l S_{ce}^{XY} \quad (3.3)$$

where the extended in-line spins are defined as  $\bar{a} = (a, j) = (a_1, a_2, \dots, a_N, j)$ , and  $\bar{b} = (g, i) =$

$(g_1, g_2, \dots, g_N, i)$ . The extended spin array  $\bar{X}$  is defined as

$$\bar{X} = \left( \begin{array}{ccc|c} x_{11} & \dots & x_{1N} & f_1 \\ \vdots & \ddots & \vdots & \vdots \\ x_{N1} & \dots & x_{NN} & f_N \\ \hline b_1 & \dots & b_N & k \end{array} \right), \quad (3.4)$$

and  $\bar{Y}$  is defined in the same way from the indices  $m, d, h$  and  $Y$ . The linear size of the corner tensor  $C$  can be increased by joining three  $P$ , three  $S$ , and a vertex (Fig.5(c))

$$C^{\bar{X}\bar{Y}\bar{Z}} = \sum_{lmn} \sum_{cd} \sum_{eh} \sum_{qr} \sum_{TUV} W_{ijklmn} P_{abcd}^n P_{efgh}^l P_{opqr}^m S_{qd}^{XT} S_{ce}^{YU} S_{hr}^{ZV} C^{TUV}. \quad (3.5)$$

The extended superscripts  $\bar{X}$ ,  $\bar{Y}$ , and  $\bar{Z}$  are defined in the same way as Eq.(3.4). In equation (3.5) we have to take care of the orientation of the surfaces  $T$ ,  $U$ , and  $V$ .

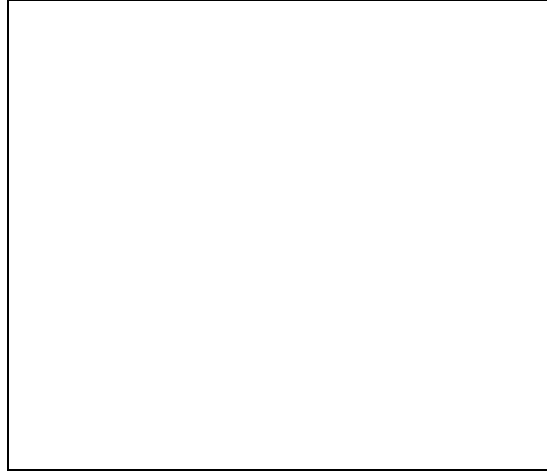


Fig. 6. The density matrix  $Q$  in Eq.(3.8) is obtained by joining two corner tensors (Eq.(3.6)) to obtain the tensor  $D$ , and then joining four of them.(Eq.(3.8))

Now we can express the partition function  $\Xi_{2N}$  of the cube with linear size  $2N$  using the corner tensors. We first join two corner tensors (Fig.5) to obtain a symmetric matrix

$$D^{(XU)(ZV)} = \sum_Y C^{XYZ} C_m^{UYV}, \quad (3.6)$$

where we regard the pair  $(ZV)$  as the column index of  $D$ , and  $(XU)$  as the row index. The tensor

$C_m$  is the mirror image of  $C$ :  $C_m^{UYV} \equiv C^{U^T Y V^T}$ . The partition function  $\Xi_{2N}$  is then expressed as

$$\Xi_{2N} = \text{Tr } D^4 = \sum_{XU} Q^{(XU)(XU)}, \quad (3.7)$$

where the matrix  $Q$  is the forth power of  $D$  (Fig.6)

$$Q^{(XU)(ZV)} = \sum_{(AB)(CD)(EF)} D^{(XU)(AB)} D^{(AB)(CD)} D^{(CD)(EF)} D^{(EF)(ZV)}. \quad (3.8)$$

The matrix  $Q$  can be seen as a density matrix for the cube, because  $\text{Tr } Q$  is the partition function  $\Xi_{2N}$ . By contracting two superscripts of  $Q$ , we obtain a density submatrix

$$\rho^{XZ} = \sum_U Q^{(XU)(ZU)}, \quad (3.9)$$

which will be used for the RG transformation for the spin array.

Let us consider a density submatrix  $\rho^{\bar{X}\bar{Z}}$  for the extended cube with size  $2(N+1)$ , where  $\bar{X}$  is the extended spin array Eq.(3.4); for a while we label the elements of  $\bar{Z}$  as

$$\bar{Z} = \left( \begin{array}{ccc|c} x'_{11} & \dots & x'_{1N} & f'_1 \\ \vdots & \ddots & \vdots & \vdots \\ x'_{N1} & \dots & x'_{NN} & f'_N \\ \hline b'_1 & \dots & b'_N & k' \end{array} \right) \quad (3.10)$$

in order to define another density submatrix. By tracing out  $N$  by  $N+1$  variables of the extended density matrix  $\rho^{\bar{X}\bar{Z}}$

$$\rho_{\bar{f}\bar{g}} = \sum_{b_i=b'_i} x_{ij}=x'_{ij} \rho^{\bar{X}\bar{Z}}, \quad (3.11)$$

where  $\bar{f} = (f_1, \dots, f_N, k)$  and  $\bar{g} = (f'_1, \dots, f'_N, k')$ , we obtain another density submatrix for the extended in-line spins. In the same way, we obtain  $\rho_{fg}$  for the in-line spins of length  $N$  —  $f = (x_{1N}, \dots, x_{NN})$  and  $g = (x'_{1N}, \dots, x'_{NN})$  — by tracing out  $N-1$  by  $N$  variables of  $\rho^{XZ}$  in Eq.(3.9).

#### §4. RG Algorithm in Three Dimension

As we have done in §2, we obtain RG transformations by way of the diagonalizations of the density submatrices. We first consider the eigenvalue relation

$$\sum_Z \rho^{XZ} U_\Psi^Z = \Lambda_\Psi U_\Psi^X, \quad (4.1)$$

where we assume the decreasing order for  $\Lambda_\Psi$ . We keep first  $m'$  eigenvalues, ( $\Psi = 1, \dots, m'$ ) and neglect the rest of relatively small ones. We then obtain the RG transformation matrix  $U_\Psi^X$ , that maps the spin array  $X$  to an  $m'$ -state block spin  $\Psi$ . For example, the corner tensor  $C^{XYZ}$  is renormalized as (Fig.7(a))

$$\tilde{C}^{\Psi\Phi\Theta} = \sum_{XYZ} U_\Psi^X U_\Phi^Y U_\Theta^Z C^{XYZ}. \quad (4.2)$$

It should be noted that under the transpose of the spin array  $X \rightarrow X^T$  the matrix  $U_\Psi^X$  transforms as  $\pm U_\Psi^X$  according to the parity of the block spin  $\Psi$ .

Let us consider another eigenvalue relation

$$\sum_g \rho_{fg} A_g^\psi = \lambda^\psi A_f^\psi \quad (4.3)$$

for the density submatrix  $\rho_{fg}$ , where  $f$  and  $g$  are in-line spins. We assume the decreasing order for  $\lambda^\psi$  as before, and we keep  $m$  numbers of large eigenvalues. ( $\psi = 1, \dots, m$ ) The matrix  $A_f^\psi$  then represent the RG transformation for the in-line spin  $f$ . For example,  $P_{abcd}^i$  is renormalized as (Fig.7(b))

$$\tilde{P}_{\alpha\beta\gamma\delta}^i = \sum_{abcd} P_{abcd}^i A_a^\alpha A_b^\beta A_c^\gamma A_d^\delta. \quad (4.4)$$

By using both  $U_\Psi^X$  and  $A_f^\psi$ , we can renormalize  $S_{ab}^{XY}$  as (Fig.7(c))

$$\tilde{S}_{\alpha\beta}^{\Psi\Phi} = \sum_{abXY} S_{ab}^{XY} A_a^\alpha A_b^\beta U_\Psi^X U_\Phi^Y. \quad (4.5)$$

As a result of RG transformations, the tensors  $P_{abcd}^i$ ,  $S_{ab}^{XY}$ , and  $C^{XYZ}$  are approximated as

$$P_{abcd}^i \sim \sum_{\alpha\beta\gamma\delta=1}^m A_a^\alpha A_b^\beta A_c^\gamma A_d^\delta \tilde{P}_{\alpha\beta\gamma\delta}^i \quad (4.6)$$

$$S_{ab}^{XY} \sim \sum_{\alpha\beta=1}^m \sum_{\Psi\Phi=1}^{m'} A_a^\alpha A_b^\beta U_\Psi^X U_\Phi^Y \tilde{S}_{\alpha\beta}^{\Psi\Phi} \quad (4.7)$$

$$C^{XYZ} \sim \sum_{\Psi\Phi\Theta=1}^{m'} U_\Psi^X U_\Phi^Y U_\Theta^Z \tilde{C}^{\Psi\Phi\Theta}. \quad (4.8)$$

For the models that have unique ground-state spin configuration, the above approximations become exact when  $T = 0$  and  $T = \infty$  even for  $m = m' = 1$ .

Now we can directly generalize the algorithm of CTMRG to 3D lattice models. The algorithm consists of the extensions for  $P_{abcd}^i$  (Eq.(3.2)),  $S_{ab}^{XY}$  (Eq.3.3)), and  $C^{XYZ}$  (Eq.(3.5)), and the RG transformations Eqs.(4.2),(4.4) and (4.5). The procedure of the renormalization group is as follows:

- (1) Start from  $N = 1$ , where all the tensors can be expressed by the Boltzmann weight  $W_{ijklmn}$ :  $P_{abcd}^i = W_{iabcd\times}$ ,  $S_{ab}^{XY} = W_{aXbY\times\times}$ , and  $C^{XYZ} = W_{ZXZY\times\times\times}$ , where the mark ‘ $\times$ ’ represents the fixed boundary spin.
- (2) Join the tensors  $W_{ijklmn}$ ,  $P_{abcd}^i$ ,  $S_{ab}^{XY}$ , and  $C^{XYZ}$  using Eqs.(3.2), (3.3), and (3.5), respectively, and obtain the extended ones  $P_{\bar{a}\bar{b}\bar{c}\bar{d}}^i$ ,  $S_{\bar{a}\bar{b}}^{\bar{X}\bar{Y}}$ , and  $C^{\bar{X}\bar{Y}\bar{Z}}$ . (Increment  $N$  by one.)
- (3) Using the extended corner tensor  $C^{\bar{X}\bar{Y}\bar{Z}}$  in Eq.(3.5), calculate the density matrix  $\rho^{\bar{X}\bar{Z}}$  via Eq.(3.9) and its submatrix  $\rho_{\bar{f}\bar{g}}$  in Eq.(3.11).
- (4) Obtain the RG transformation matrix  $U_\Psi^{\bar{X}}$  and  $A_a^\alpha$  using Eqs.(4.1) and (4.3), respectively. We keep  $m'$  states for  $\Psi$ , and  $m$  states for  $\alpha$ .

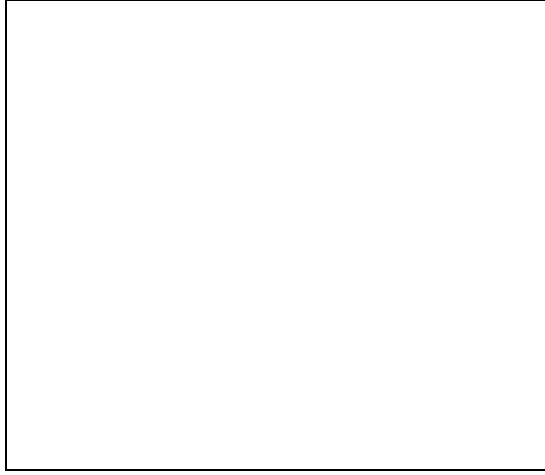


Fig. 7. The renormalized tensors (a)  $\tilde{P}_{\alpha\beta\gamma\delta}^i$  in Eq.(4.4), (b)  $\tilde{S}_{\alpha\beta}^{\Psi\Phi}$  in Eq.(4.5), and (c)  $\tilde{C}^{\Psi\Phi\Theta}$  in Eq.(4.2). The greek letters  $\alpha, \beta, \gamma$ , and  $\delta$  denote  $m$ -state renormalized in-line spins, and the capital ones  $\Psi, \Phi$ , and  $\Theta$  denote  $m'$ -state renormalized spin arrays.

- (5) Apply the RG transformations to the extended tensors to obtain  $\tilde{P}_{\alpha\beta\gamma\delta}^i$  (Eq.(4.4)),  $\tilde{S}_{\alpha\beta}^{\Psi\Phi}$  (Eq.(4.5)), and  $\tilde{C}^{\Psi\Phi\Theta}$  (Eq.(4.2)).
- (6) Goto the step (2) and repeat the procedures (2)-(5) for the renormalized tensors  $\tilde{P}$ ,  $\tilde{S}$ , and  $\tilde{C}$ .

Every time we extend the tensors in the step (2) the system size — the linear dimension of the cube — increases by 2. After the step (3) we can obtain the lower bound of the partition function by taking the trace of the density submatrix  $\Xi_{2(N+1)} = \text{Tr } \rho^{\bar{X}\bar{Z}} = \text{Tr } \rho_{\bar{f}\bar{g}}$ . We stop the iteration when the partition function per vertex converges. Since the extended spin array  $\bar{X}$  of the density matrix  $\rho^{\bar{X}\bar{Z}}$  contains the original (unrenormalized) spin variable, we can directly calculate the local energy and the order parameter.<sup>29)</sup>

Let us apply the above algorithm to the 3D Ising model. The model is equivalent to the 64-vertex model whose vertex weight is given by

$$W_{ijklmn} = \sum_{\sigma=\pm 1} U_{\sigma i} U_{\sigma j} U_{\sigma k} U_{\sigma l} U_{\sigma m} U_{\sigma n}, \quad (4.9)$$

where  $U_{\sigma i}$  is unity when  $\sigma = i$ , and is  $e^K + \sqrt{e^{2K} - 1}$  when  $\sigma \neq i$ . The parameter  $K$  denotes the inverse temperature  $J/k_B T$ . For this model the initial conditions for step (1) are slightly modified as

$$P_{abcd}^i = U_{\times i} U_{\times a} U_{\times b} U_{\times c} U_{\times d}$$

$$\begin{aligned} S_{ab}^{XY} &= U_{\times X} U_{\times Y} U_{\times a} U_{\times b} \\ C^{XYZ} &= U_{\times X} U_{\times Y} U_{\times Z}, \end{aligned} \quad (4.10)$$

where ‘ $\times$ ’ represent the boundary Ising spin. (The modification is nothing but the change in normalizations.) We impose ferromagnetic boundary condition  $\times = 1$ . As a trial calculation we keep only two states for both in-line spins ( $m = 2$ ) and spin arrays ( $m' = 2$ ); when  $m' = 2$  the parity of the renormalized spin array  $\Psi$  in Eq.(4.1) is always even. Figure 8 shows the calculated spontaneous magnetization. Because of the smallness of  $m$  and  $m'$ , the transition temperature  $T_c$  is over estimated, where the feature is common to the Klamers-Wannier approximation.<sup>1)</sup>

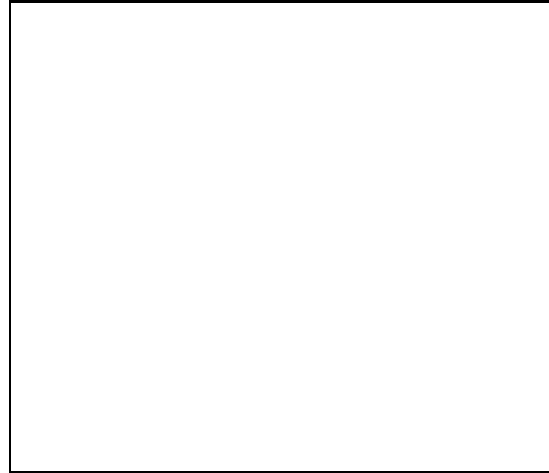


Fig. 8. Calculated spontaneous magnetization of the 3D Ising model when  $m = m' = 2$ . The arrow shows the true  $T_c$ .

Compare to the CTMRG algorithm for 2D classical systems, the above RG algorithm for 3D system requires much more computational time. The reason is that after the step (2) the extended in-line spin  $\bar{f}$  becomes  $2m$ -state, and the extended spin array  $\bar{X}$  becomes  $2m^2m'$ -state; in order to obtain  $\rho^{\bar{X}\bar{Z}}$  in the step (3) we have to create a matrix  $D^{(\bar{X}\bar{U})(\bar{Z}\bar{V})}$  by Eq.(3.6), whose dimension is  $4m^4m'^2$ . For the simplest (non-trivial) case  $m = m' = 2$  the dimension is already 256.

## §5. Conclusion and discussion

We have explained a way of generalizing the RG algorithm of CTMRG<sup>28,29)</sup> to 3D classical models, focusing on the construction of the density matrix from eight corner tensors. The RG transformations are obtained through the diagonalizations of the density matrices. As far as we

know it is the first generalization of the infinite-system density matrix algorithm<sup>15, 16)</sup> to 3D classical systems.

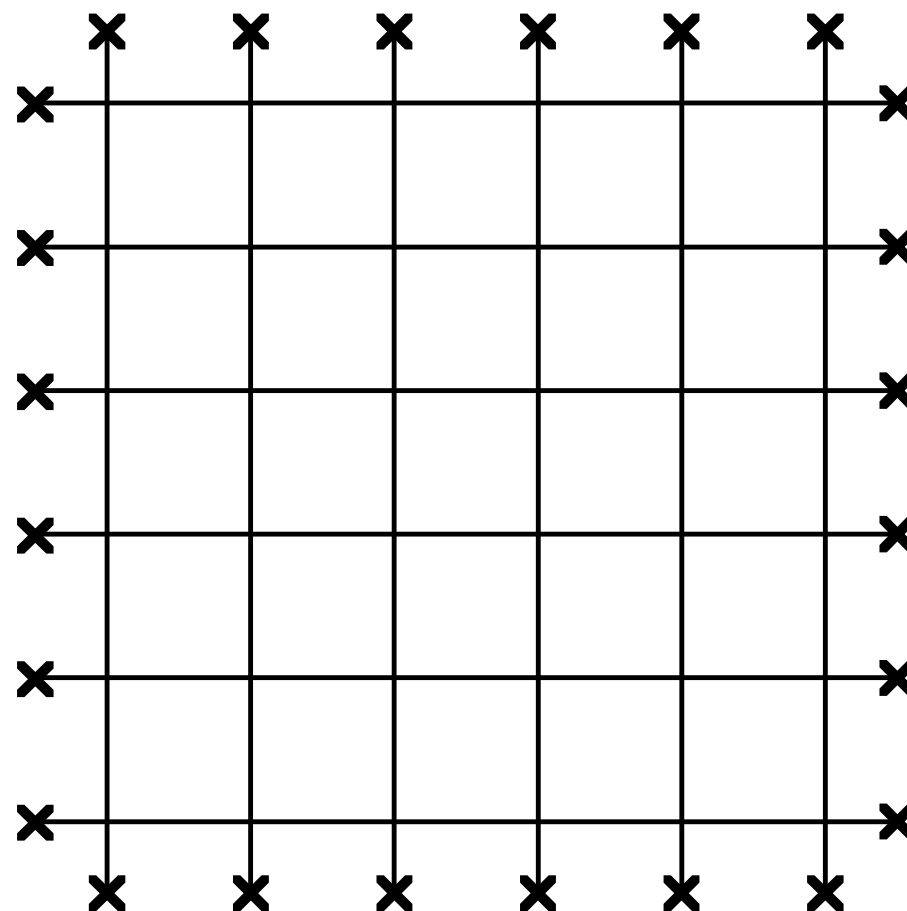
From the computational view point, the calculation in 3D is far more heavy than that of CTMRG in 2D; we have to improve the numerical algorithm in 3D for realistic use. What we have done is to approximate the eigenstate of a transfer matrix in 3D as a two-dimensional product of renormalized tensor  $\tilde{P}$  (Eq.(4.4)); the most important process is to improve the tensor elements in  $\tilde{P}$  so that the variational partition function is maximized. The improvement of tensor product state for 1D quantum system proposed by Dukelsky et. al.,<sup>26, 27)</sup> where their algorithm does not explicitly require the density matrix, may of use to reduce the numerical effort in three dimension.

The authors would like to express their sincere thanks to Y. Akutsu, M. Kikuchi, for valuable discussions. T. N. is greatful to G. Sierra about the discussion on the matrix product state. K. O. is supported by JSPS Research Fellowships for Young Scientists. The present work is partially supported by a Grant-in-Aid from Ministry of Education, Science and Culture of Japan. Most of the numerical calculations were done by NEC SX-4 in computer center of Osaka University.

---

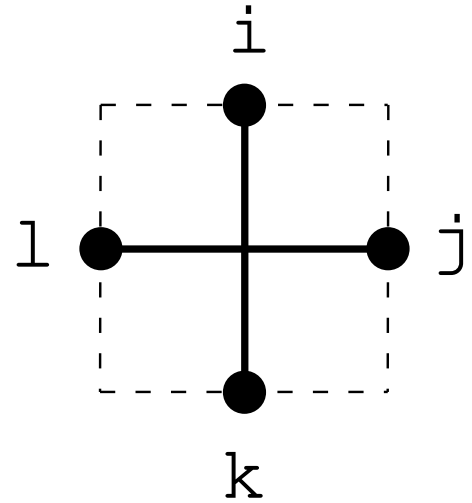
- [1] H. A. Kramers and G. H. Wannier, Phys. Rev. **60** (1941) 263.
- [2] R. Kikuchi, Phys. Rev. **81** (1951) 988.
- [3] H. A. Bethe: Proc. Roy. Soc. **A150** (1935) 552.
- [4] R. J. Baxter: J. Math. Phys. **9** (1968) 650 .
- [5] R. J. Baxter: J. Stat. Phys. **19** (1978) 461.
- [6] R. J. Baxter: *Exactly Solved Models in Statistical Mechanics* (Academic Press, London, 1982) p.363.
- [7] N. P. Nightingale and H. W. Blöte: Phys. Rev. **B33** 659.
- [8] I. Affleck, T. Kennedy, E. H. Lieb, and H. Tasaki: Phys. Rev. Lett. **59** (1987) 799.
- [9] M. Fannes, B. Nachtergale, and R. F. Werner: Europhys. Lett. **10** (1989) 633.
- [10] M. Fannes, B. Nachtergale, and R. F. Werner: Commun. Math. Phys. **144** (1992) 443.
- [11] M. Fannes, B. Nachtergale, and R. F. Werner: Commun. Math. Phys. **174** (1995) 477.
- [12] A. Klümper, A. Schadschneider and J. Zittartz: Z. Phys. **B87** (1992) 281.
- [13] H. Niggemann, G. Uimin, and J. Zittartz: Z. Phys. **B104** (1997) 103-110.
- [14] H. Takasaki and T. Nishino: unpublished.
- [15] S. R. White: Phys. Rev. Lett. **69** (1992) 2863.
- [16] S. R. White: Phys. Rev. **B48** (1993) 10345.
- [17] S. Östlund and S. Rommer: Phys. Rev. Lett. **75** (1995) 3537.
- [18] S. Rommer and S. Östlund: Phys. Rev. **B55** (1997) 2164.
- [19] S. R. White and D. A. Huse: Phys. Rev. **B48** (1993) 3844.
- [20] K. Hida: J. Phys. Soc. Jpn. **65** (1996) 895.
- [21] G. Sierra and M. A. Martín-Delgado: *Strongly Correlated Magnetic and Superconducting Systems*, (Springer Berlin, 1997), and references there in.
- [22] T. Nishino, J. Phys. Soc. Jpn. **64**, No.10 (1995) 3598.
- [23] Enrico Carlon and Andrej Drzewiński: Phys. Rev. Lett. **79** (1997) 1591.
- [24] Enrico Carlon and Andrej Drzewiński: cond-mat/9709176.
- [25] G. Sierra, M. A. Martín-Delgado, J. Dukelsky, S. R. White, and D. J. Scalapino: cond-mat/9707335.

- [26] J. Dukelsky, M. A. Martín-Delgado, T. Nishino, and G. Sierra: cond-mat/9710310.
- [27] J. M. Roman, G. Sierra, J. Dukelski, and M. A. Martín-Delgado: cond-mat/9802150.
- [28] T. Nishino and K. Okunishi: J. Phys. Soc. Jpn. **65** (1996) 891.
- [29] T. Nishino and K. Okunishi: J. Phys. Soc. Jpn. **66** (1997) 3040.
- [30] T. Nishino and K. Okunishi: to be published in J. Phys. Soc. Jpn. **67** (1998); cond-mat/9711214.
- [31] The generalization of CTMRG to asymmetric vertex models is straight forward.
- [32] To introduce such a symmetry is not a over simplification. For example, the  $d = 3$  Ising model can be expressed as a three-dimensional 64-vertex model. (See Eqs.(4.9)-(4.12))

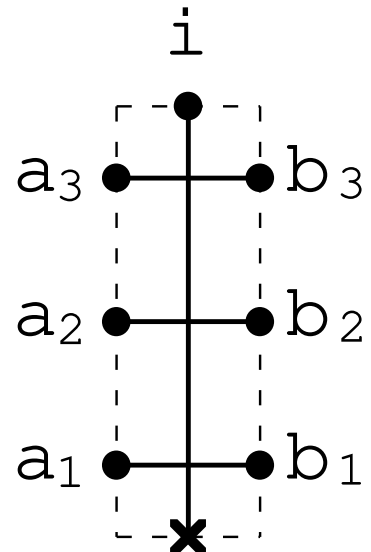


- Fig.1 -

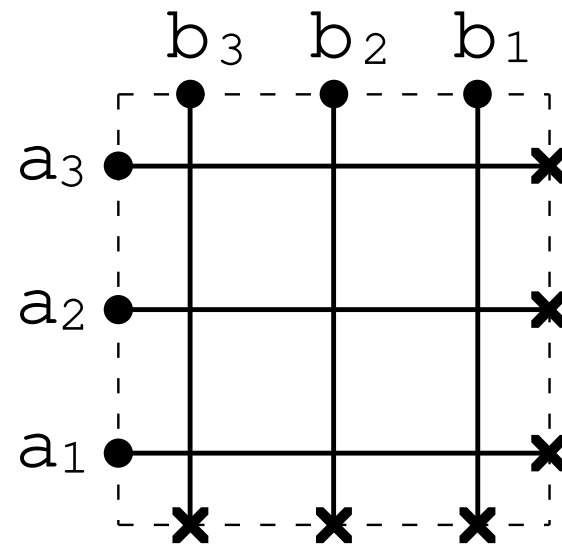
**T. Nishino  
K. Okunishi**



( a )



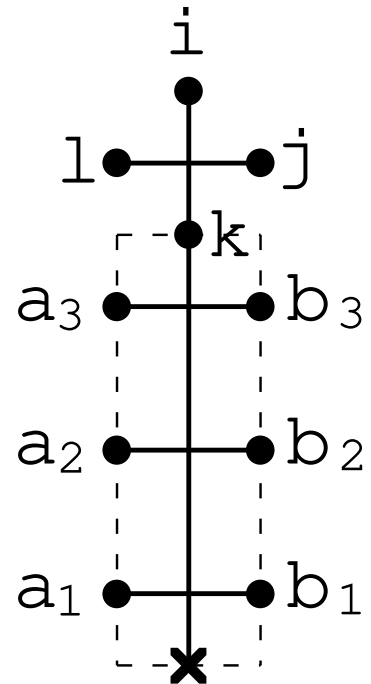
( b )



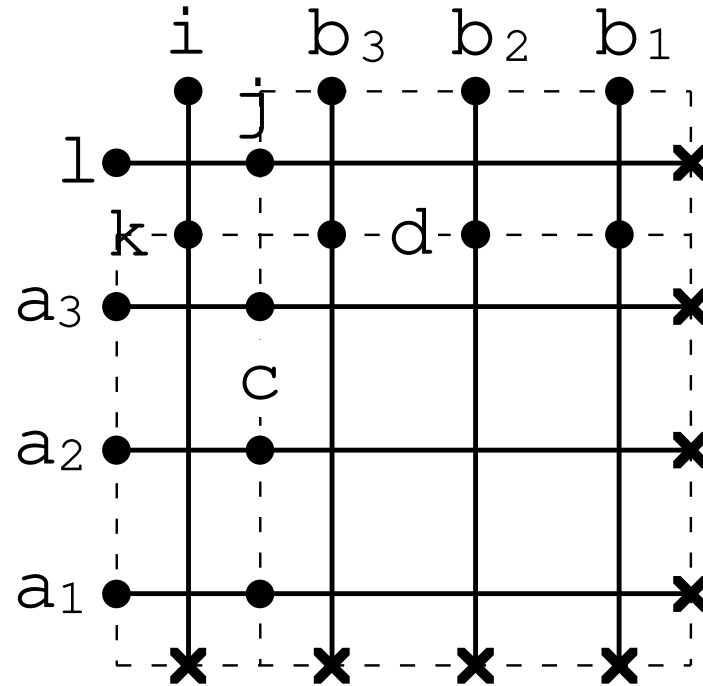
( c )

- Fig.2 -

**T. Nishino**  
**K. Okunishi**



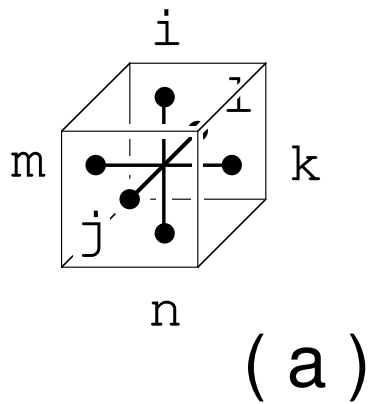
( a )



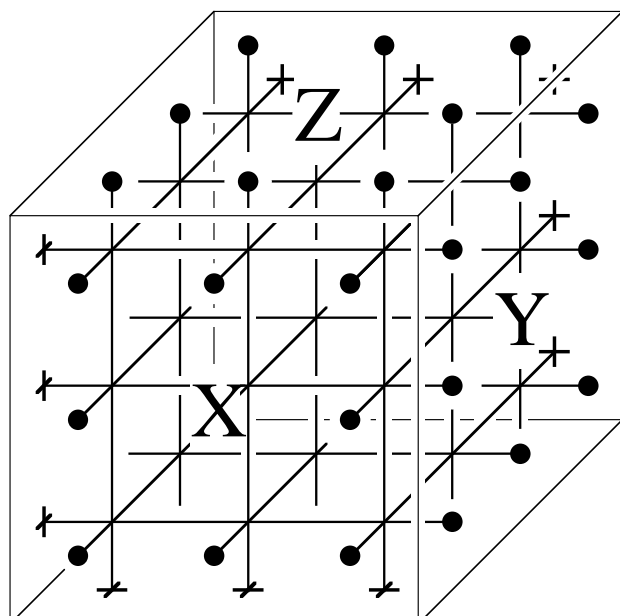
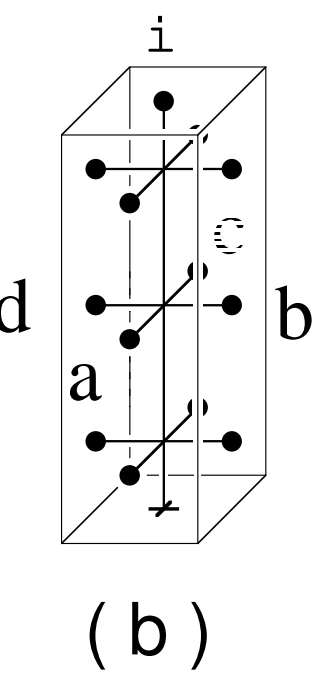
( b )

- Fig.3 -

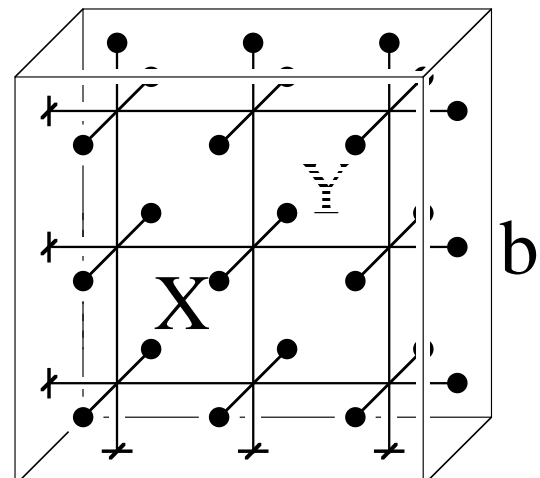
**T. Nishino**  
**K. Okunishi**



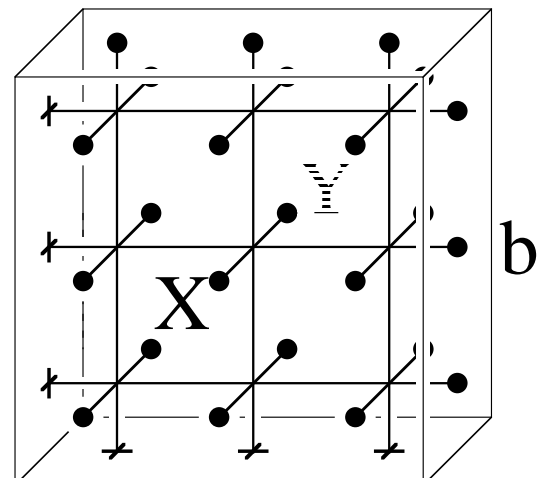
- Fig. 4 -



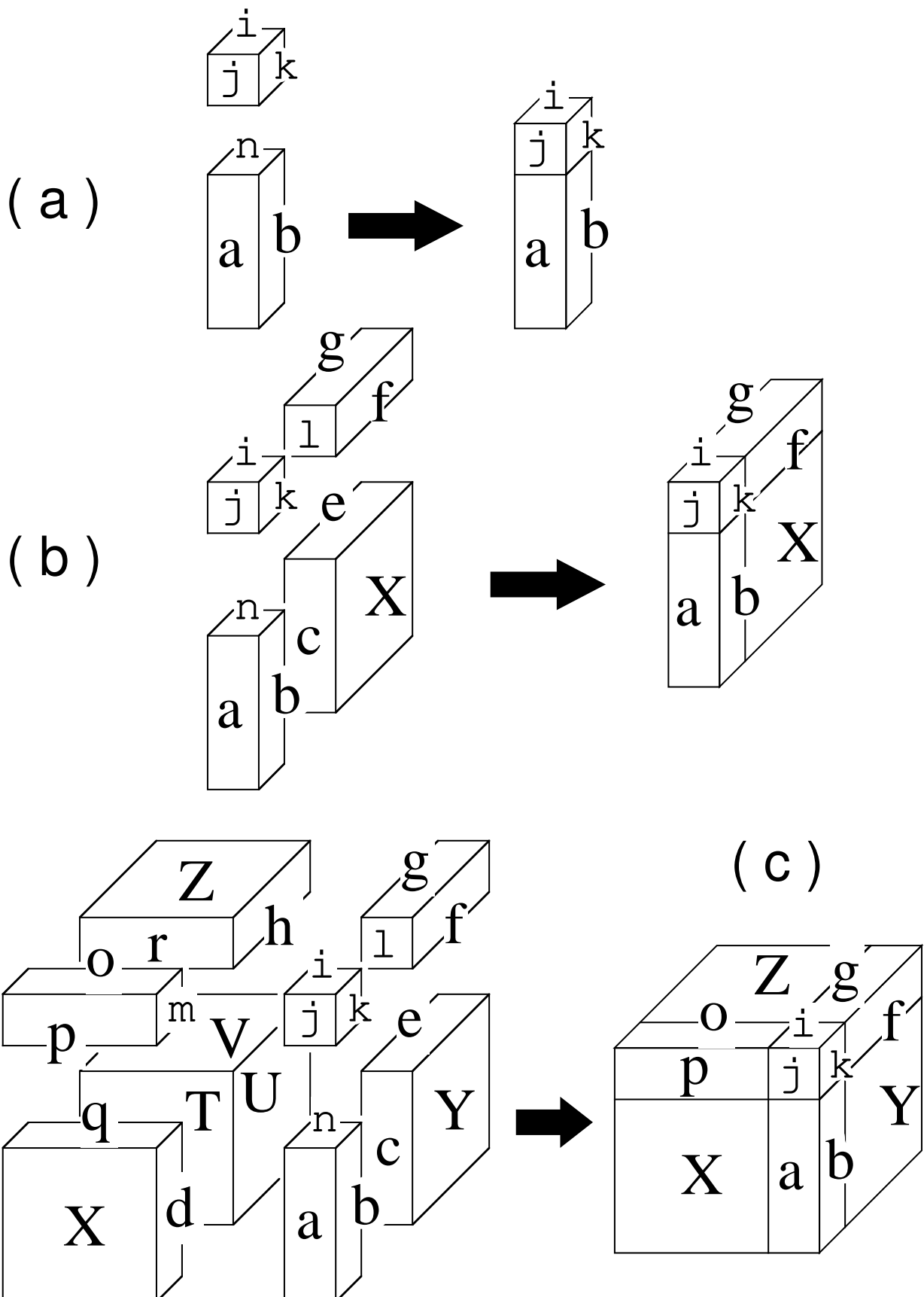
**T. Nishino**  
**K. Okunishi**



( c )

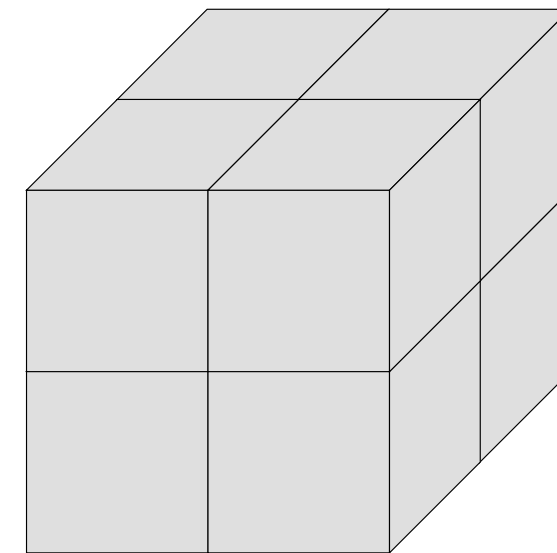
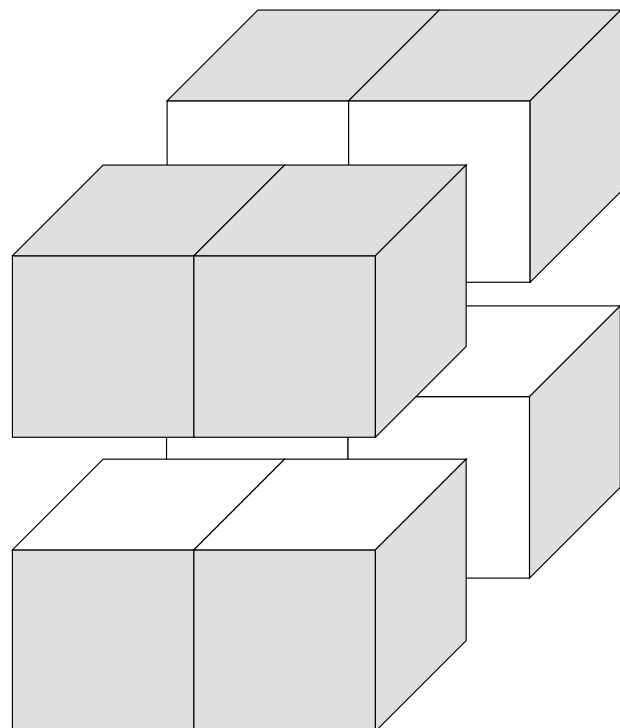
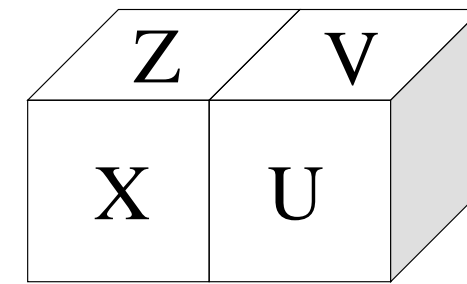
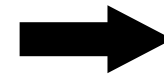
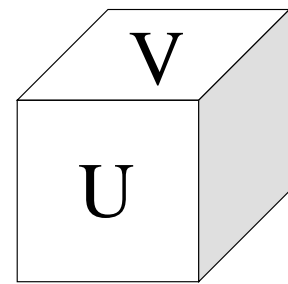
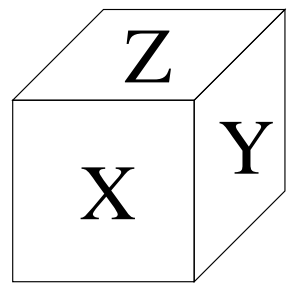


( d )



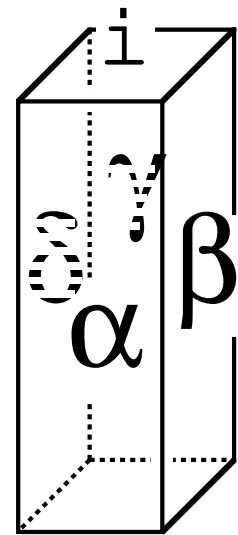
- Fig. 5 -

**T. Nishino**  
**K. Okunishi**

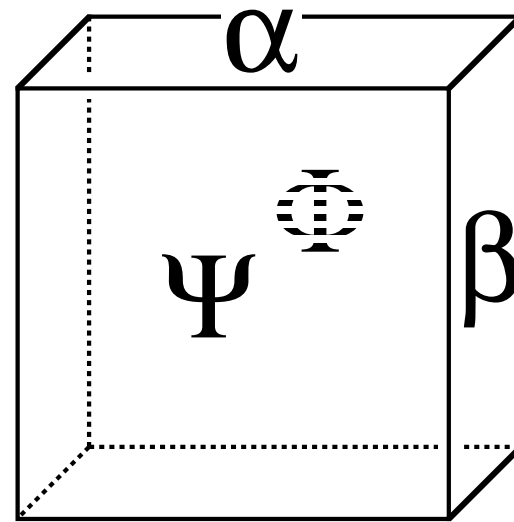


- Fig. 6 -

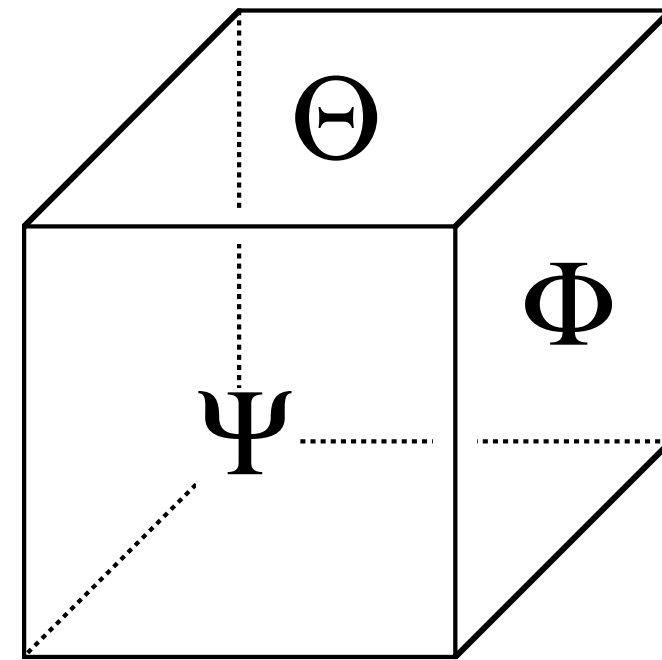
**T. Nishino  
K. Okunishi**



$\tilde{P}$   
( a )



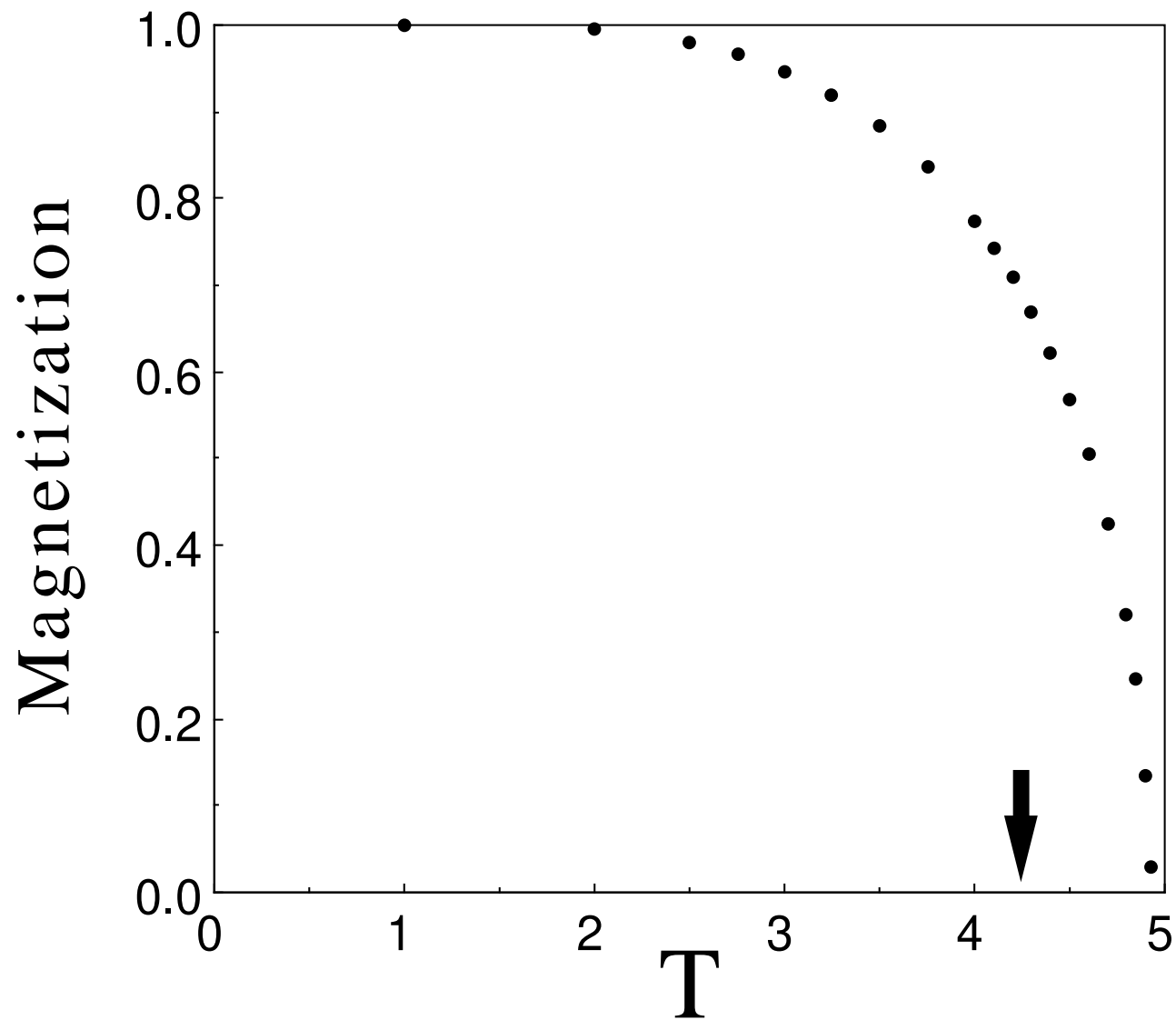
$\tilde{S}$   
( b )



$\tilde{C}$   
( c )

- Fig. 7 -

**T. Nishino  
K. Okunishi**



- Fig.8 -

**T. Nishino**  
**K. Okunishi**